

## CFD investigation of cross-flow effects on fire-wind enhancement

E. Eftekharian<sup>1</sup>, M. Ghodrat<sup>1</sup>, R.H. Ong<sup>2</sup>, Y. He<sup>1</sup> and K.C.S. Kwok<sup>2,1</sup>

<sup>1</sup>Center for Infrastructure Engineering, School of Computing Engineering and Mathematics  
 Western Sydney University, Penrith, NSW, 2751, Australia

<sup>2</sup>School of Civil Engineering,  
 The University of Sydney, NSW, Australia

### Abstract

Investigation of fire-wind (fire cross-wind) interaction is highly instrumental in dissecting the potential effects of bushfire attacks on buildings. The increase of free-stream wind velocity downstream of the fire source due to the interaction of wind and fire is referred as fire-wind enhancement which has been recognized as one of the destructive consequences of bushfire-wind interaction. Although occurrence of the fire-wind enhancement phenomenon has been reported in previous studies, the mechanisms and contributing factors affecting the phenomenon have not been reported in the literature. This study applies Computational Fluid Dynamics (CFD) technique to fundamentally investigate the effects of cross-wind on fire-wind enhancement. Fire-FOAM solver which is based on OpenFOAM platform was used to solve thermo-fluid governing equations. A module has been added to the solver to extract different components of flow acceleration and the corresponding fire-induced flow momentum. Experimental data of buoyant diffusion flame was used to validate the numerical model. A selected range of simulation scenarios with different free-stream wind velocities under constant fire intensity has been performed to identify the effects of free-stream wind velocity on fire-wind enhancement. The outcome of the research indicated that as a result of interaction of cross-wind and fire, a longitudinal (horizontal) favorable pressure gradient is generated which leads to enhancement of wind downstream of the fire. It was also shown that the normalized fire-induced pressure gradient decreases when free-stream wind velocity increases. Therefore, for constant fire intensity, the flow field with a higher free-stream wind velocity undergoes a lower enhancement.

### Introduction

Interaction of wind and fire is a two-way problem. That is wind causes a change of fire plume geometrical features and also fire affects flow (wind) aerodynamic properties. Many studies have focused on the effects of wind on fire plume geometrical properties [3]. Fire plume tilt angle and flame length were investigated in [4,5].

As for the effects of fire on the wind, it was experimentally shown that interaction of wind and fire can result in the increase of wind velocity downstream of the fire [2]. Thermal expansion and low-density area within the plume region were found to be the reasons for distortion in the velocity profile [12]. Therefore, the knowledge of thermal and geometrical details of plume region will help better understanding of the phenomenon.

Fire-wind enhancement is one of the mechanisms of bushfire attacks. Lambert [7] and McRae et al [9] reported that wind can be intensified due to the interaction with bushfire and cause damages to buildings and vegetations. He et al [1] and Kwok et al [6] numerically investigated bushfire-wind interaction and showed that it can potentially enhance the near ground wind

velocity downstream of the bushfire source up to 50%. They showed that accompanied by the increase of wind velocity, bushfire-wind interaction results in an increase of turbulence and wind gust. Coanda effects were postulated to be the reason why the wind is enhanced downstream of the bushfire source. As a result of the increase in wind velocity due to fire-wind-interaction, the pressure coefficient around the buildings downstream of the bush-fire source was shown to be increased.

There are two controlling factors in the process of fire-wind interaction: one is the longitudinal momentum flux which is determined by the wind velocity for given ambient air density; and the other is the buoyancy flux which is determined by gravitational acceleration and density difference between the momentum flow and fire induced buoyancy flow. The focus of the current study is to employ Computational Fluid Dynamics technique to fundamentally investigate the effects of wind velocity on the fire-wind enhancement phenomenon, whereas the effects of buoyancy flux would be reported elsewhere.

### Numerical Approach

FireFOAM, a solver of OpenFOAM platform was employed to simulate the interaction of fire and wind. OpenFOAM is an open-source CFD code with different solvers for different thermo-fluid application problems. FireFOAM uses large eddy simulation (LES) to capture turbulent structures of the flow. Continuity, momentum, energy, state and species equations solved by FireFOAM are as below:

$$\frac{\partial \bar{\rho}}{\partial t} + \frac{\partial (\bar{\rho} \tilde{u}_i)}{\partial x_i} = 0 \quad (1)$$

$$\frac{\partial (\bar{\rho} \tilde{u}_i)}{\partial t} + \frac{\partial (\bar{\rho} \tilde{u}_i \tilde{u}_j)}{\partial x_j} = \frac{\partial}{\partial x_j} \left[ \bar{\rho} (v + v_t) \left( \frac{\partial \tilde{u}_i}{\partial x_j} + \frac{\partial \tilde{u}_j}{\partial x_i} - \frac{2}{3} \frac{\partial \tilde{u}_k}{\partial x_k} \delta_{ij} \right) - \bar{p} \delta_{ij} \right] + \bar{\rho} g_i \quad (2)$$

$$\frac{\partial (\bar{\rho} \tilde{h})}{\partial t} + \frac{\partial (\bar{\rho} \tilde{u}_j \tilde{h})}{\partial x_j} = \frac{D\bar{p}}{Dt} + \frac{\partial}{\partial x_j} \left[ \bar{\rho} \left( D_c + \frac{v_t}{Pr_t} \right) \left( \frac{\partial \tilde{h}}{\partial x_j} \right) + \dot{q}''' - \nabla \cdot \dot{q}_r'' \right] \quad (3)$$

$$\frac{\partial \bar{\rho} \tilde{Y}_m}{\partial t} + \frac{\partial (\bar{\rho} \tilde{u}_j \tilde{Y}_m)}{\partial x_j} = \frac{\partial}{\partial x_j} \left[ \bar{\rho} + \left( D_c + \frac{v_t}{Pr_t} \right) \frac{\partial \tilde{Y}_m}{\partial x_j} \right] + \omega_m \quad (4)$$

$$\bar{p} = \bar{\rho} R \tilde{T} \quad (5)$$

where the superscripts “-” and “~” indicate spatial and Favre filtering.  $P$  is static pressure (Pa),  $h$  is total enthalpy (kJ/m<sup>3</sup>),  $Y_m$

is mass fraction of species  $m$ ,  $g$  is gravitational acceleration ( $\text{m/s}^2$ ),  $\nu, \nu_t, D_c, R, Pr, \delta$  and  $\omega_m$ , are laminar viscosity ( $\text{m}^2/\text{s}$ ), turbulent viscosity ( $\text{m}^2/\text{s}$ ), laminar diffusion coefficient, gas constant, Prandtl number, Kronecker delta and production/sink rate of species  $m$  due to gas reaction respectively.  $\dot{q}'''$  is heat release rate per unit volume ( $\text{W/m}^3$ ) from a chemical reaction and  $\dot{q}_r''$  is the total radiation emission intensity ( $\text{W/m}^2$ ) of the gas mixture. 20 % of radiant fraction was used in this study. FireFOAM uses PISO scheme to couple velocity and pressure field. First order upwind was used as the differencing scheme and kEq model was used to model sub-grid scale turbulent structures. Eddy Dissipation Model (EDM) was applied as the combustion model.

Momentum equation (Eq. (2)) can be written based on the flow acceleration as:

$$\vec{a} = \frac{D\vec{u}}{Dt} = \frac{-\nabla p}{\rho} + \vec{g} + \frac{\Phi}{\rho} \quad (6)$$

In which  $\vec{a}$  is the flow acceleration,  $u$  is the flow velocity,  $\nabla p$  is pressure gradient ( $\text{N/m}^2.\text{s}$ ),  $\rho$  is density ( $\text{m}^3/\text{s}$ ),  $\vec{g}$  is gravitational acceleration and  $\Phi$  is the viscous shear stress tensor. Eq. (6) shows that the flow acceleration can be decomposed in three components, namely, pressure acceleration ( $\frac{-\nabla p}{\rho}$ ), gravitational acceleration ( $\vec{g}$ ) and viscous acceleration ( $\frac{\Phi}{\rho}$ ). In the longitudinal direction along which wind blows, the gravitational acceleration is absent and flow acceleration is attributable to pressure gradient and the viscous shear stress only.

### Model Description and Boundary Conditions

The computational domain consists of a rectangular box with the dimension of  $34 \times 9 \times 15\text{m}$  as shown in Figure 1. A line source of fire with the width of  $0.3\text{m}$  is introduced  $3\text{m}$  downstream of the domain inlet. Methane was used as the fuel in the burner (fire source) to generate  $7\text{ MW/m}^2$  heat release rate.

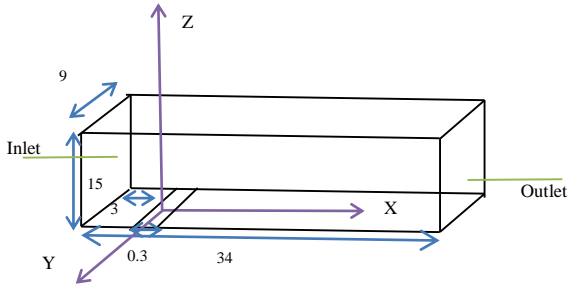


Figure 1. A schematic view of the computational domain.

Atmospheric boundary layer (ABL) condition with power-law velocity profile as in Eq.(7) was considered for the domain inlet.

$$U(Z) = U_{ref} \left( \frac{Z}{Z_{ref}} \right)^\alpha \quad (7)$$

in which  $U_{ref}$  and  $Z_{ref}$  are respectively the reference velocity and reference height (3 m). Three different wind reference velocities (3 m/s, 4.5 m/s and 6 m/s) were used to investigate the effects of wind velocity on fire wind enhancement. Adiabatic boundary condition was used for the domain base. The value of the power  $\alpha$  is determined according to the terrain category and for the current study it is taken to be 0.16. The two dimensional vortex method [8] was used to take into account turbulent structures at the domain inlet. The initial temperature and velocity inside the whole domain were set to be 300 K and 0 m/s respectively.

No-slip wall boundary condition was prescribed for the domain base, while slip boundary was suggested for the domain sides. To treat wall-bounded flow in the domain base, wall-function [11] was used. Open boundary condition was used for the domain top. This boundary allows the flow to freely get in or out of the computational domain. Pressure-outlet boundary was applied to the domain outlet.

### Grid sensitivity analysis

Three different grids including course (300 k), medium (2.4 million) and fine (7 million) were tested and a negligible difference ( $<1\%$ ) in longitudinal velocity distribution was found between the results of medium and fine grid, while the corresponding difference between the coarse and medium grid is about 7%. Hence, the medium grid was chosen for simulation in this study.

### Validation

Experimental data of buoyant diffusion flame reported by McCaffery [9], was used to validate the numerical model of the current study. McCaffery [9] used methane to produce buoyant diffusion fire plume in still conditions. The considered fire heat release rate is  $Q=58\text{ kW}$ . The grid size similar to that suggested in [13] was used for validation in this study. Figure 2 compares the normalized vertical velocity profile at the centerline of the fire plume between the results of the current study, numerical results of Wang et al [13] and experimental data produced by McCaffery [9]. It is shown that there is a reasonably good agreement between the current numerical results and the experimental data of McCaffery [9].

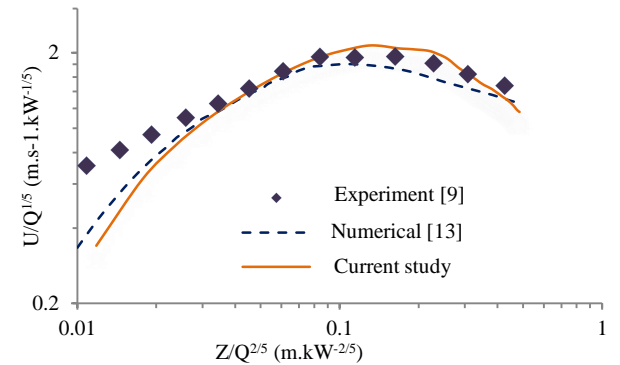


Figure 2 Comparison of numerical results of the current study with the numerical results of Wang et al [13] and experimental data produced by McCaffery [9].

### Results and discussion

Simulated flow duration for all simulation cases is 24 s. The first 12 second is considered as the transition period for the simulation to reach a quasi-steady condition. Therefore, all the presented results are based on the average of the last 12 seconds of the quasi-steady period.

Figure 3 depicts longitudinal velocity distribution at the horizontal plane ( $Y=0$  in Figure 1). It is shown that longitudinal velocity is considerably enhanced downstream of the fire source. For the case of  $U_{ref} = 3\text{ m/s}$ , for instance, the longitudinal velocity in the plume region downstream of the fire source is more than doubled that of the freestream. The reason is that due to the interaction of wind and fire, a favourable longitudinal pressure gradient is generated (as shown in Figure 4) within the

plume region (low density area), which according to Eq. (6) accelerates the flow and causes wind enhancement.

therefore makes a greater contribution in total horizontal acceleration and enhancement of wind.

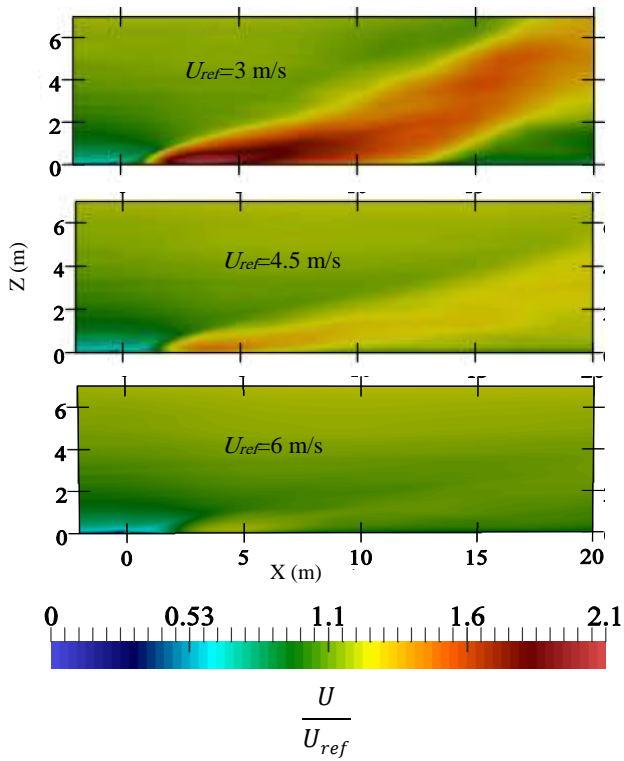


Figure 3. Distribution of normalised time-averaged longitudinal velocity in a vertical plane passing the domain centreline ( $Y=0$  in Figure 1) for different upstream wind velocities.

However, the level of enhancement changes with the change in the free-stream wind velocity. Figure 3 shows that under constant fire intensity, wind velocity enhancement decreases as the free-stream wind velocity increases. The reason is that the corresponding normalised longitudinal fire-induced pressure gradient reduces as free-stream wind velocity increases, as shown in Figure 4. This is mainly because fire intensity, which is the main cause of generating pressure gradient, remains the same for the three simulations. Consequently, with the increase of wind velocity, the incoming flow momentum is increasing while the fire-induced pressure gradient does not vary significantly, culminating in a lower impact on the wind velocity downstream of the fire.

Figure 3 also shows that for all free-stream wind velocities, the flow is attached to the ground immediately downstream of the fire source and it starts to lift up from the ground in further downstream. This is the manifestation of Coanda effects which have also been observed in the previous studies [1,6].

Figure 5 shows temperature distributions at  $Y=0$ . In contrast to the normalised longitudinal velocity and pressure gradient distribution (shown in Figure 3 and Figure 4), normalised temperature distribution is not significantly affected by changing free stream wind velocity. This is mainly because density is a thermodynamic property of the flow which is mainly controlled by the source of heat release rate (fire) rather than wind.

Figure 6 shows different components of fire-induced horizontal acceleration (i.e. total, pressure and viscous) for the case with  $U_{ref}=3\text{m/s}$ . Figure 6 shows that pressure acceleration is dominant

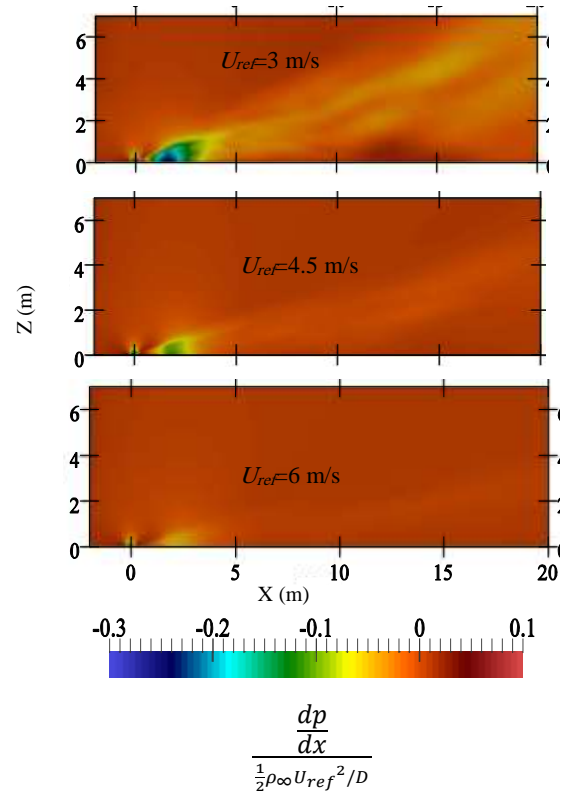


Figure 4 Distribution of normalised time-averaged longitudinal pressure gradient in a vertical plane ( $Y=0$  in Figure 1) for different upstream wind velocities.

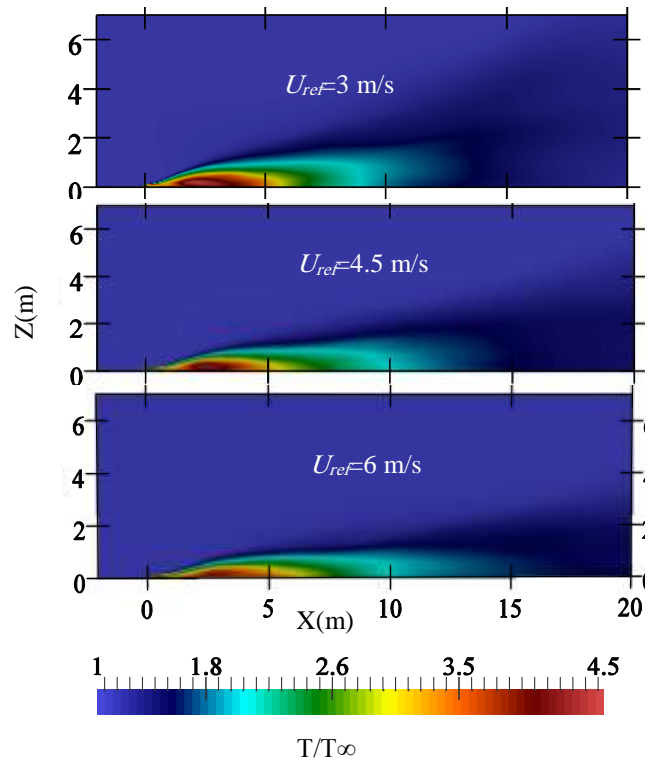


Figure 5 Distribution of normalised time-averaged temperature in a vertical plane, passing the domain centreline, ( $Y=0$  in Figure 1) for different upstream wind velocities ( $T_{\infty}=300\text{ K}$ ).

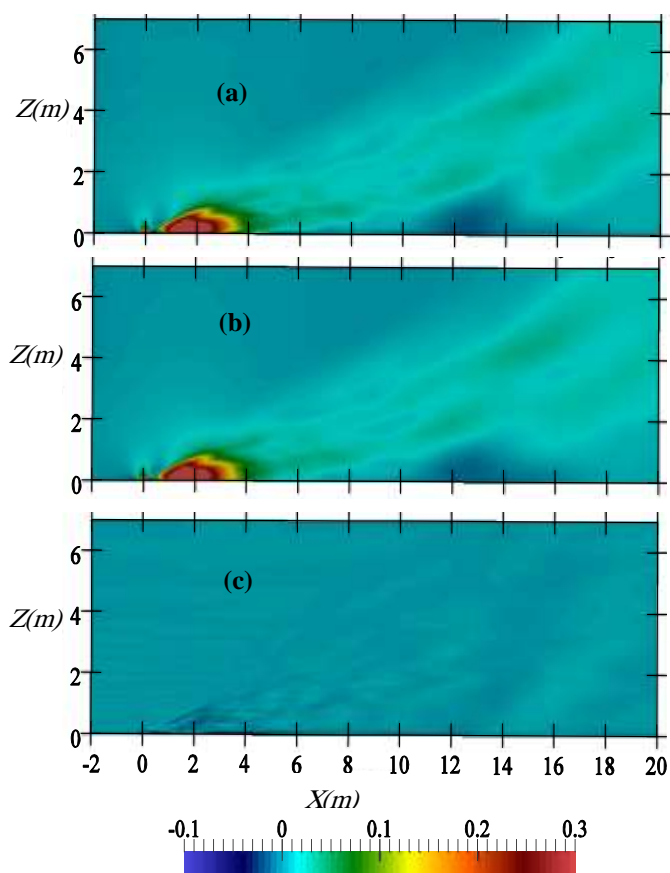


Figure 6 distribution of normalised time-averaged horizontal (a) total acceleration  $\left(\frac{-\frac{dp}{dx} + \phi}{\frac{1}{2}\rho U_{ref}^2/D}\right)$ , (b) pressure acceleration  $\left(\frac{-\frac{dp}{dx}}{\frac{1}{2}\rho U_{ref}^2/D}\right)$  and (c) viscous acceleration  $\left(\frac{\phi}{\frac{1}{2}\rho U_{ref}^2/D}\right)$  for the case with  $U_{ref} = 3$  m/s.

## Conclusions

This study used Computational Fluid Dynamics to investigate the effects of wind velocity on fire wind enhancement. The results of this study can be concluded as below:

- Interaction of fire and wind causes generation of a longitudinal (horizontal) pressure gradient that accelerates the free-stream wind velocity and cause fire wind enhancement.
- With the increase of wind velocity under a constant fire intensity, normalised longitudinal pressure gradient and wind velocity enhancement decreases, while density distribution remains almost unchanged.
- Enhancement of the longitudinal velocity happens in the fire plume region which is more inclined toward the ground when wind velocity increases.

## Acknowledgement

This project is financially supported by Australian Research Council grant ARC-DP160103248. We would also like to acknowledge the OpenFOAM and FM-Global foundation that provide an open-source CFD platform.

## References

- [1] He, Y, Kwok, K, Douglas, G & Razali, I 2011, 'Numerical Investigation of Bushfire-Wind Interaction and its Impact on Building Structure', *Fire Safety Science*, vol. 10, pp. 1449-62.
- [2] Hirano, T & Kinoshita, M 1975, 'Gas velocity and temperature profiles of a diffusion flame stabilized in the stream over liquid fuel', *Symposium (International) on Combustion*, vol. 15, no. 1, pp. 379-87.
- [3] Hu, L 2017, 'A review of physics and correlations of pool fire behaviour in wind and future challenges', *Fire Safety Journal*, vol. 91, no. Supplement C, pp. 41-55.
- [4] Hu, L, Liu, S, de Ris, JL & Wu, L 2013, 'A new mathematical quantification of wind-blown flame tilt angle of hydrocarbon pool fires with a new global correlation model', *Fuel*, vol. 106, pp. 730-6.
- [5] Hu, L, Wu, L & Liu, S 2013, 'Flame length elongation behavior of medium hydrocarbon pool fires in cross air flow', *Fuel*, vol. 111, pp. 613-20.
- [6] Kwok, K, He, Y & Douglas, G 2012, 'Bushfire-enhanced wind load on structures', *Proceedings of the Institution of Civil Engineers-Engineering and Computational Mechanics*, vol. 165, no. 4, pp. 253-63.
- [7] Lambert, K 2010, *Extreme bushfire/firestorm impact and the bush/urban interface*, Black Saturday 7th February 2009, 2009 Victorian Bushfires Royal Commission, 13th Feb. 2014, <[www.royalcommission.vic.gov.au/Submissions/SubmissionDocuments/SUBM-002-059-0366\\_01\\_R.pdf](http://www.royalcommission.vic.gov.au/Submissions/SubmissionDocuments/SUBM-002-059-0366_01_R.pdf)>.
- [8] Mathey, F, Cokljat, D, Bertoglio, JP & Sergent, E 2006, 'Assessment of the vortex method for large eddy simulation inlet conditions', *Progress in Computational Fluid Dynamics*, vol. 6, no. 1-3, pp. 58-67.
- [9] McCaffrey, BJ 1979, *Purely Buoyant Diffusion Flames: Some Experimental Results*, vol. NBSIR 79-1910.
- [10] McRae, RHD, Sharples, JJ, Wilkes, SR & Walker, A 2013, 'An Australian pyro-tornadogenesis event', *Natural Hazards*, vol. 65, no. 3, pp. 1801-11.
- [11] Spalding, D 1961, 'A single formula for the "law of the wall"', *Journal of Applied Mechanics*, vol. 28, no. 3, pp. 455-8.
- [12] Volchkov, ÉP, Terekhov, VI & Terekhov, VV 2004, 'Flow Structure and Heat and Mass Transfer in Boundary Layers with Injection of Chemically Reacting Substances (Review)', *Combustion, Explosion and Shock Waves*, vol. 40, no. 1, pp. 1-16.
- [13] Wang, Y, Chatterjee, P & de Ris, JL 2011, 'Large eddy simulation of fire plumes', *Proceedings of the Combustion Institute*, vol. 33, no. 2, pp. 2473-80.